Technical Note
radphi-1999-901

Comparison of Expected and Measured Trigger Rates during 1999 Radphi Commissioning

Richard Jones

University of Connecticut, Storrs, CT

Sept 17, 1999

Abstract

In a previous report a set of predicted rates for the Radphi trigger following the barrel upgrade were put forward, based upon a Monte Carlo simulation. Since that time the experiment has undergone a commissioning run in which the new detector and trigger electronics were used for the first time under conditions like those under which we expect to run. This report compares the predicted to the measured rates, and demonstrates that the experiment is capable of taking data with reasonable efficiency at a tagger rate of 50MHz.

Table 1: The rates in all levels of the Radphi trigger from the front end to the tape. The measured values were taken during 1999 running with 5.5GeV electrons at 125nA and a double radiator each of nominal $1 \cdot 10^{-4}$ radiation lengths. This corresponds to $5 \cdot 10^{7}$ tagged photons per second, to within 10%. The predicted values are taken from Table 3 of Ref. [1].

signal	scaler	corrected	predicted
tagger *or*	30 MHz	50 MHz	48 MHz
CPV *or*	33 MHz	40 MHz	67 MHz
UPV *or*	550 KHz		750 KHz
BSD layer 1	4.1 MHz	4.7 MHz	3.9 MHz
BSD layer 2	2.4 MHz	2.6 MHz	2.0 MHz
BSD layer 3	1.5 MHz	1.6 MHz	1.2 MHz
BSD $1 \cdot 2 \cdot 3$	900 KHz		440 KHz
$BSD \cdot \overline{UPV}$	800 KHz		390 KHz
$BSD \cdot \overline{UPV} \cdot TAG$	750 KHz		150 KHz

1 Method

The Radphi commissioning run of 1999 was presented several new conditions over what had been available during previous parasitic run periods. The first was the upgraded barrel detector that replaces the former recoil proton annulus with a full barrel calorimeter/veto. The second is a new level-2 trigger that enables running without an online charged-particle veto that was formerly limiting our rate capability. The third is the availability of photons up to 5.5GeV in energy. After setup and debugging for a period in parasitic mode with CLAS, we were granted control of the beam and were able during this period to raise the photon beam intensity to the level at which we expect to run. The measurements that were taken at that time are the subject of the following report. The expected and measured rates are in good agreement, showing that the detector is well reproduced in the Monte Carlo. Based upon the new measurements, the parameters that describe the trigger have been refined and improved estimates of the signal yield are presented as a function of beam intensity.

2 Results

The important rates that enter the Radphi trigger are shown in Table 1. The first column shows the number that is read from the instrumentation, for example a scaler. The value in the second column, if any, is the corrected rate in the case that the scaler is affected by an internal dead time. This is only important for rates above several MHz. The predictions in the last column are copied from Table 3 of Ref. [1].

The comparison between predicted and measured rate for the taggerOR simply reflects the choice of beam current. All of the other comparisons are a check of our understanding of the apparatus. There is excellent agreement for the cpv (charged particle veto) and upv (upstream veto) in spite of the fact that these counters are sensitive to the tune of the machine. The predicted values were calculated assuming an ideal (zero-emittance) electron beam. The calculation assumed that the CLAS liquid hydrogen target is present and full, whereas during the measurement it was present but empty. The difference between the calculation and the measurement can be taken as an estimate of the effect of filling the CLAS target on the charged-particle rates in Radphi.

There is an overall scale factor in the predicted BSD (barrel scintillator detector) rates that depends on the setting of the BSD discriminator. In Ref. [1] the discriminator setting was taken to fall at the maximum of the minimum-ionizing peak in the scintillators. Figures in that report show the difference in the energy loss spectra for recoil protons and the minimum-ionizing background from electromagnetic showers. Those figures can be compared with Figs. 1-2 below. The Monte Carlo did not include the effects of attenuation in the scintillator paddles. The fact of attenuation implies that one must chose a position along the length of the paddles where to set the threshold to the minimum-ionzing maximum, and that where that peak falls relative to the threshold will depend on polar angle, or z. The overlaps of the barrel scintillators allow them to be divided longitudinally into pixels of about 10cm in length. Pixel number increases with z from 0 (upstream) to 7 (downstream). Pixels 0 and 7 are half-pixels. To be safe, we chose to set the threshold

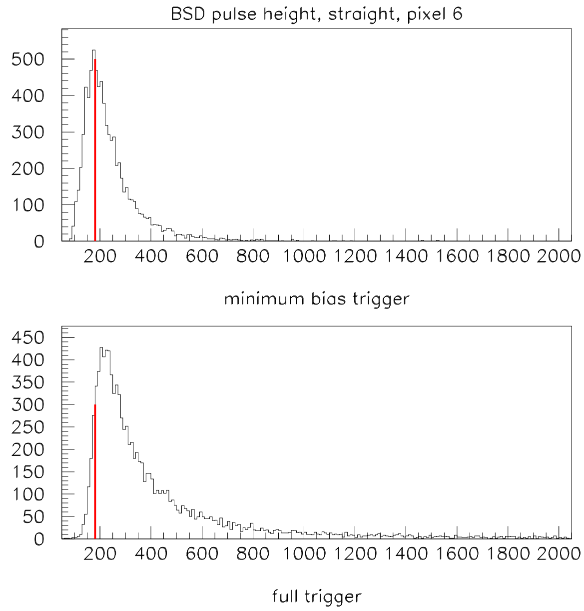

Figure 1: Pulse height spectrum for *pixel* (triple-coincidence between three overlapping counters) hits in the BSD, for different trigger conditions. Pixel 6 is located near the downstream end of the barrel, in the vicinity of 30^o polar angle.The upper plot is mainly electromagnetic background, whereas the lower plot is mainly recoil protons. The red line indicates where the threshold was set for normal running.

in the middle of the MIP peak for pixel 6 near the downstream end, as shown in Fig. 1. The upper plot includes all triple-coincidences between the *OR*s of the three BSD layers, with the BSD threshold set low to reveal the minimum-biased spectrum. Most of these hits are MIP background. The lower plot shows the same spectrum taken with the threshold set at the operating point (indicated by the red line) and a trigger that requires a large energy deposit in the lead glass. Most of these hits are presumably recoil protons.

Fig. 2 shows the same pair of spectra for hits in pixel 2, towards the upstream end of the counter. Here one can see the increased pulse height relative to pixel 6, which results in a decreased discrimination against background for upstream pixels, over what was expected without attenuation in the Monte Carlo. As can be seen in Fig. 3, the background rates are strongly peaked downstream, which means that the sacrifice in background rejection at the upstream end of the counter does not have too large an effect on our overall level 1 trigger rate. The three independent layers are hence 25% over the predicted rates, which can be roughly cubed to obtain the factor of 2 in the measured triple-coincidence rate over the prediction. We were careful during the test to ere on the side of a low threshold, knowing that for the test we could raise it offline. With the threshold taken into account, the agreement with Monte Carlo is very good. At this point a more careful study can be made using the t-slope for particular reactions and varying the target diameter, to determine the threshold that optimizes between dead-time and acceptance.

The tagging coincidence window was set to 30ns during the test run. This contrasts with the 10ns gate that was assumed in the Monte Carlo calculation. At present the alignment between the different tagging channels and BSD elements does not allow an efficient tag with a gate as narrow as 10ns. For the purposes of accidentals subtraction it may prove valuable to keep the online gate window somewhat larger than the actual coincidence peak. With some effort cutting cables, we expect to be able to reduce this gate width to 20ns.

The comparison between measured and predicted values for the higher levels of the Radphi trigger are shown in Table 2. Here the measurements are much better than the predictions, which compensates for the excess at level 1 over expectation. The reason for the large errors in the calculation is that this is the first time we have run the Radphi trigger without a charged-particle veto at level 1, and it turns out that estimates of leakage from charged-particle events through the upper-level trigger decisions were far too conservative. The net effect is that the rate of events to tape is an order of magnitude lower than predicted.

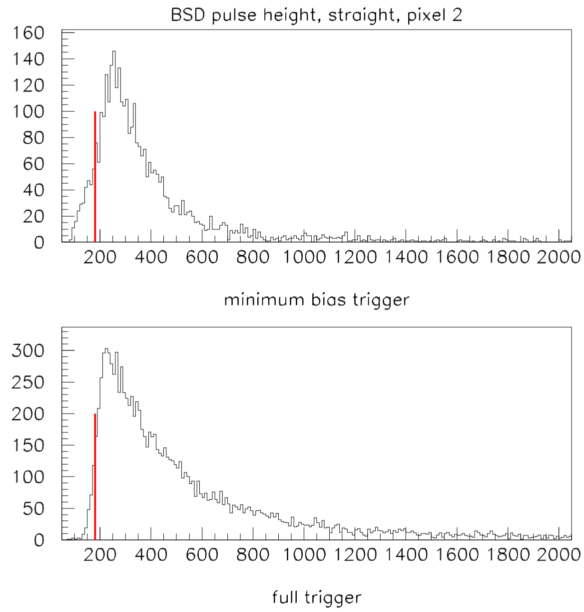

Figure 2: Pulse height spectrum for *pixel* (triple-coincidence between three overlapping counters) hits in the BSD, for different trigger conditions. Pixel 2 is located near the upstream end of the barrel, in the vicinity of 60^o polar angle.The upper plot is mainly electromagnetic background, whereas the lower plot is mainly recoil protons. The red line indicates where the threshold was set for normal running.

Table 2: Measured and predicted rates in the upper levels of the Radphi trigger, under the same conditions as shown in Fig. 1. The dead-time per event are average values under high-intensity conditions.

signal	measured	predicted
level 1 trigger	300 KHz	73 KHz
level 2 trigger	6.2 KHz	8.3 KHz
level 3 trigger	80 Hz	1.0 KHz
level 2 dead time	1.7 μs/event	1.2 μs/event
level 3 dead time	11 μs/event	14 μs/event
daq dead time	300 μs/event	300 μs/event
total live time	40% @ 80Hz	50% @ 1KHz

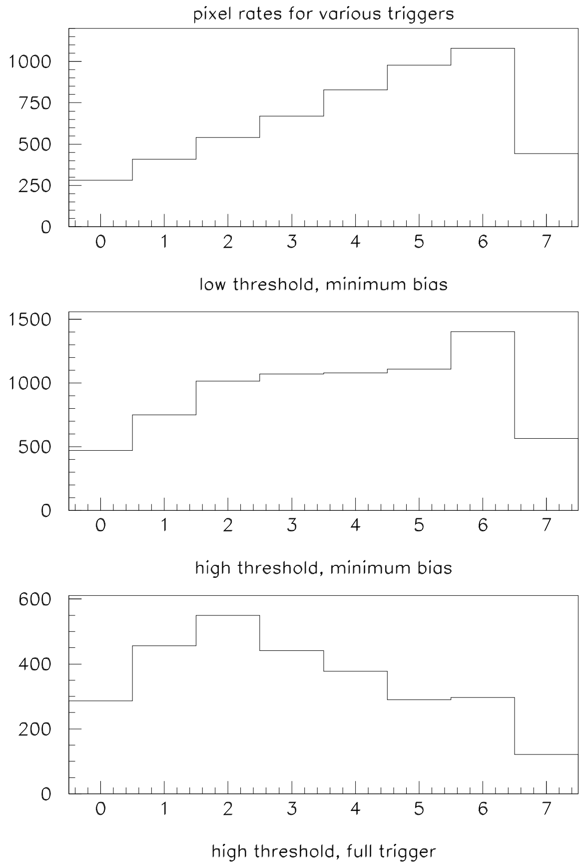

Figure 3: Pixel hit distribution for various triggers, ranging from minimum-biased at low threshold (top) to the physics trigger (bottom). The distribution of minimum biased hits background is peaked towards forward angles, as expected for electromagnetic background. The bottom profile agrees well with the recoil proton angular distribution from diffractive photoproduction. The middle plot shows what comes in at trigger level 1, which is intermediate between the two.

Table 3: Parameters supplied as input to the model, calibrated using the rates measured at 125nA and 5.5GeV endpoint in 1999.

parameter	value		method
r_T	$4.00 \cdot 10^5$	/s/nA	fit to TDC data
r_R	$5.00 \cdot 10^3$	/s/nA	fit to TDC data
r_U	$4.5 \cdot 10^4$	/s/nA	fit to TDC data
r_C	$3.0 \cdot 10^5$	/s/nA	fit to TDC data
t_T	$3.0 \cdot 10^{-8}$	s	TDC spectra
t_C	$0.0 \cdot 10^{-8}$	s	(disabled)
d_T	$1.0 \cdot 10^{-8}$	s	fit to scaler data
d_C	$4.0 \cdot 10^{-9}$	s	fit to scaler data
d_2	$1.1 \cdot 10^{-5}$	s	measured on scope
d_{DAQ}	$3.0 \cdot 10^{-4}$	s	measured on scope
f_s	$5.5 \cdot 10^{-3}$		measured at low rates
f_n	$5.5 \cdot 10^{-1}$		from TDC spectra
f_c	$1.1 \cdot 10^{-2}$		measured at low rates
f_p	$3.3 \cdot 10^{-1}$		from TDC spectra
f_{2s}	$1.0 \cdot 10^{-1}$		from TDC spectra
f_{2n}	$8.0 \cdot 10^{-3}$		from TDC spectra
f_{2c}	$3.2 \cdot 10^{-1}$		from TDC spectra
f_{2p}	$3.3 \cdot 10^{-2}$		from TDC spectra
f_{3s}	$0.5 \cdot 10^{-2}$		from TDC spectra
f_{3n}	$0.1 \cdot 10^{-3}$		from TDC spectra
f_{3c}	$0.9 \cdot 10^{-2}$		from TDC spectra
f_{3p}	$2.8 \cdot 10^{-4}$		from TDC spectra

The majority of the experimental dead-time comes from the level-2 logic. The excess dead-time at level-2 per event over the 1.2μs that was foreseen was inserted to give adequate time for the high-resolution TDC to fast-clear. A simple rearrangement of our electronics is discussed below that will allow us to reduce this dead-time by a factor of 2.

3 Dead-time and Yield vs Beam Intensity

To map out the dependence on beam intensity of the yield of true-tagged events, use is made of a model of the Radphi trigger that is described in detail elsewhere Ref. [2]. Without further comment I reproduce here Table 1 from that note, with values of the parameters updated based upon the measurements taken in 1999. The fact that several of the background suppression factors in Table 3 are much smaller than initially supposed explains why the rate of events to tape is so much smaller than predicted.

The model gives good agreement with the measured rates at 125nA and 20nA taken during July-August 1999. Using the model it is now possible to extrapolate to beam currents where there are no measurements, and decide what is the optimum beam current at which to run. The experimental live-time fraction is shown in Fig. 4 under the conditions of 1999 running. The dead-time contributions from each of DAQ, level 3 and level 2 are shown by the stacked curves. Level 2 is clearly the most important. As mentioned above, we have a scheme in hand that will enable us to reduce the level 2 dead-time per event by a factor of 2. The new live-time curve from this modification resulting resulting from this modification is shown in Fig. 5.

The bottom line is determined by the number of true-coincidence events being written to tape per second. This quantity is plotted vs beam current if Fig. 6. The point represented by $5 \cdot 10^7$ photons/s is 125nA in this figure. The curve is still rising at this current, indicating that the trigger is still some distance from saturation.

From these results we conclude that the Radphi trigger is now capable of taking data at the luminosity listed in the proposal. Some improvements over the performance obtained in 1999 can yet be obtained by

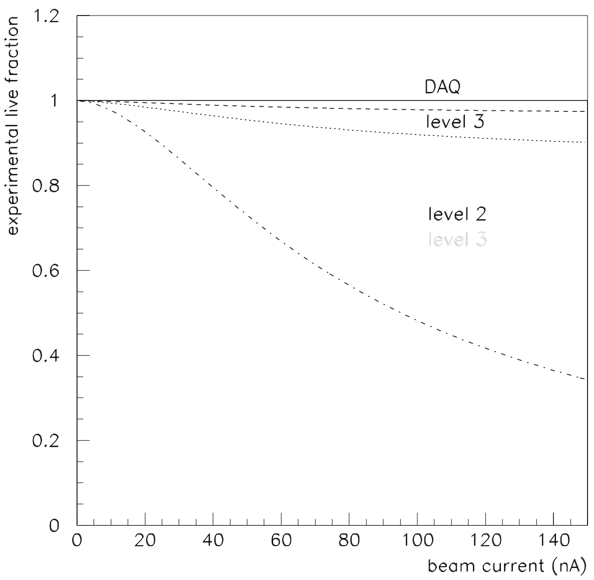

Figure 4: Calculated live time vs beam current under the conditions for 1999 running, calibrated using the measurements described in this report.

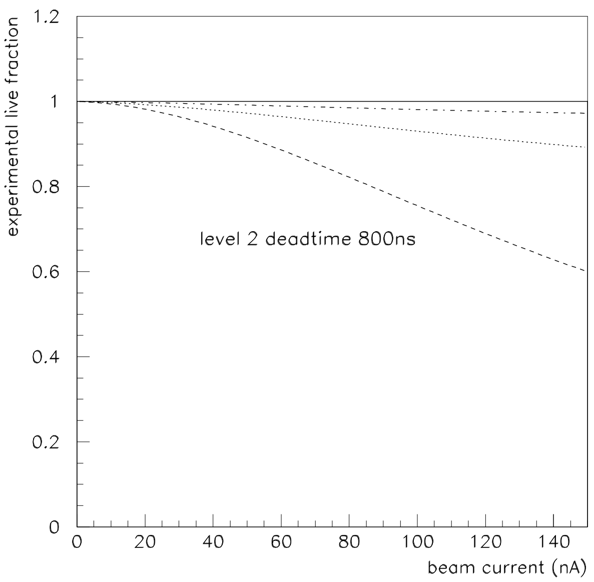

Figure 5: Improved live-time vs beam current profile, after reducing the level-1 dead time as described in the text.

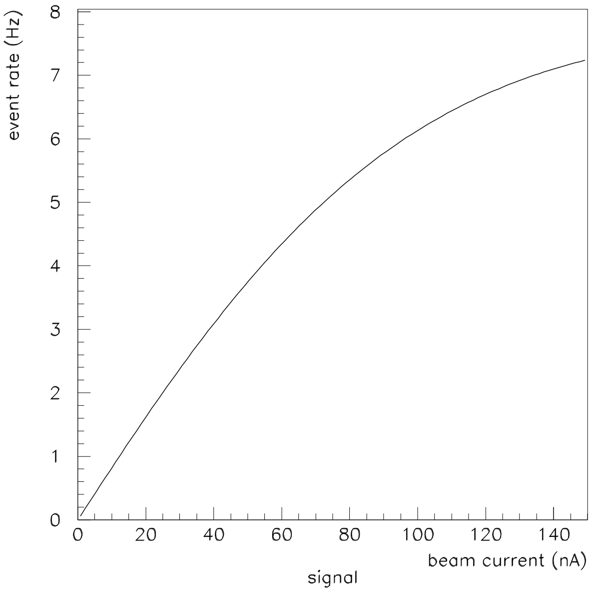

Figure 6: Rate of writing signal events to tape vs beam current under conditions foreseen for running during Y2K. Signal events are defined as those generated from a photon within the tagging energy range, and which did not include a charge track.

streamlining the level 2 trigger and optimizing the relative timing of the tagger and BSD counters. A further study is planned to investigate how much acceptance can be gained by reducing the diameter of the target. Using the data on tape from the 1999 run it will be possible to refine the choice of the BSD threshold to maintain good acceptance for protons while improving somewhat the background rejection at level 1.

References

[1] "Predicted Rates in Radphi following the Barrel Upgrade", R.T. Jones, Technical Note *radphi-1999-601*, June 16, 1999.

[2] "Prospects for running Radphi at design luminosity in 1999", R.T. Jones, Technical Note *radphi-1998-901*, October 24, 1999.